Food Chemistry: X 12 (2021) 100138

Contents lists available at ScienceDirect

Food Chemistry: X

journal homepage: www.sciencedirect.com/journal/food-chemistry-x

Use of jackfruit leaf (*Artocarpus heterophyllus* L.) protein hydrolysates as a stabilizer of the nanoemulsions loaded with extract-rich in pentacyclic triterpenes obtained from *Coccoloba uvifera* L. leaf

Carolina Calderón-chiu [a], Montserrat Calderón-santoyo [a], Simone Damasceno-gomes [b], Juan Arturo Ragazzo-Sánchez [a,*]

[a] *Laboratorio Integral de Investigación en Alimentos, Tecnológico Nacional de México/Instituto Tecnológico de Tepic, Av. Tecnológico #2595, Col. Lagos del Country, Tepic, Nayarit C.P. 63175, México*

[b] *Center of Exact and Technological Sciences, State University of West Paraná (UNIOESTE), Cascavel, Brazil*

ARTICLE INFO

Keyword:
Pentacyclic triterpenes extract
Nanoemulsion O/W
Jackfruit leaf
Leaf protein hydrolysates
Coccoloba uvifera L.

Chemical compounds used in this article:
Pancreatin (EC 232-468-9)
Sodium hydroxide (NaOH, PubChem CID: 14798)
Hydrochloric acid (HCl, PubChem CID: 313)
Hexane (PubChem CID: 8058)
Methanol (PubChem CID: 887).

ABSTRACT

This study aimed to evaluate the encapsulating potential of a jackfruit leaf protein hydrolysate, through obtaining pentacyclic triterpenes-rich extract loaded nanoemulsion. Response surface methodology (RSM) was used to optimize the conditions to obtain an optimal nanoemulsion (NE-Opt). The effect of protein hydrolysate concentration (0.5–2%), oil loaded with extract (2.5–7.5%), and ultrasound time (5–15 min) on the polydispersity index (PDI) and droplet size of the emulsion (D[3,2] and D[4,3]) was evaluated. RSM revealed that 1.25% protein hydrolysate, 2.5% oil, and ultrasound time of 15 min produced the NE-Opt with the lowest PDI (0.85), D[3,2] (330 nm), and D[4,3] (360 nm). Encapsulation efficiency and extract loading of the NE-Opt was of 40.15 ± 1.46 and 18.03 ± 2.78% respectively. The NE-Opt was relatively stable during storage (at 4 and 25 °C), pH, temperature, and ionic strength. Then, the protein hydrolysate could be used as an alternative to conventional emulsifiers.

Introduction

Coccoloba uvifera L. (sea grape) is a fruit rich in phytochemicals like polyphenols, flavonoids, and anthocyanins, which give it antioxidant properties (Ramos-Bell, Calderón-Santoyo, Barros-Castillo, & Ragazzo-Sánchez, 2020), while *Coccoloba uvifera* L. leaf extract is a source with high content of pentacyclic triterpenes (PTs) such as lupeol, α- and β-amyrin (Ramos-Hernández, Calderón-Santoyo, Navarro-Ocaña, Barros-Castillo, & Ragazzo-Sánchez, 2018). PTs are high-value biological compounds (HVBC) that, in recent years, have aroused interest due to their comprehensive spectrum of biological activities (Salvador et al., 2017). Among them, the anticancer activity of PTs is the interest. In particular, sea grape leaf extract has fractions with antimutagenic activity and antiproliferative capacity, which were mainly attributed to the lupeol content (Ramos-Hernández, Calderón-Santoyo, Burgos-Hernández, García- Romo, Navarro-Ocaña, Burboa-Zazueta, Sandoval-Petris, & Ragazzo- Sánchez, 2021).

Studies have revealed that PTs can modulate a wide range of multiple targets and signaling pathways involved in the survival, progression, and resistance of cancer. Nevertheless, the low water solubility, rapid metabolism, and low bioavailability of some pentacyclic triterpenes make their application difficult (Salvador et al., 2017). In this regard, encapsulation technologies, such as oil in water (O/W) nanoemulsions (NEs) offer great potential to maintain/release HVBC with low water solubility and ensure controlled release. This approach increases the solubility in water and enhances the bioavailability of lipophilic HVBC.

O/W nanoemulsions are colloidal dispersions composed of two immiscible liquids (oil and water phase), in which the oil phase is dispersed in the aqueous phase in the form of surfactant-stabilized oil droplets with diameters of 20–500 nm (Karami, Saghatchi Zanjani, & Hamidi, 2019). The O/W interface of the food-grade emulsions is frequently stabilized by proteins due to their amphiphilic character. Currently, the food industry mainly uses animal protein as emulsifiers. However, higher consumption of animal protein leads to increased

* Corresponding author.
E-mail addresses: simone.gomes@unioeste.br (S. Damasceno-gomes), jragazzo@ittepic.edu.mx (J.A. Ragazzo-Sánchez).

https://doi.org/10.1016/j.fochx.2021.100138
Received 13 August 2021; Received in revised form 23 September 2021; Accepted 1 October 2021
Available online 7 October 2021

greenhouse gas emissions, biodiversity loss, and climate change. In this regard, the use of plant proteins to encapsulate HVBC by emulsions has been proposed, since is relatively profitable and an alternate to the use of animal proteins in the food, cosmetic, and drug sectors (Sharif et al., 2018).

For this reason, studies on plant proteins from unconventional sources and their hydrolysates have increased, since it was shown that protein hydrolysates have improved interfacial diffusivity than the native protein. Enzymatic hydrolysis is a safe, simple, and inexpensive method to enhance emulsifying and antioxidant activities of plant proteins (Liu, Bhattarai, Mikkonen, & Heinonen, 2019). The improvement in emulsifying properties due to partial hydrolysis of the proteins is due to the increase in solubility, the revelation of hidden hydrophobic groups, the increase in surface hydrophobicity, and the reduction of molecular weight, which allows obtaining protein fragments with better adherence to the O/W interface (Lam & Nickerson, 2013).

Protein hydrolysates from rice glutelin (Xu et al., 2016), fava bean (Liu et al., 2019), rice bran (Zang, Yue, Wang, Shao, & Yu, 2019), among others, could be a suitable alternative to animal proteins and be used as emulsifiers. These studies demonstrated that vegetable protein hydrolysates have good emulsifying properties. Moreover, that the production of highly functional hydrolysates from agro-industrial by-products can be a feasible alternative to produce food ingredients and a circular economy strategy for reducing waste. However, further research including these protein hydrolysates in real food, cosmetic and pharmaceutical systems was recommended.

Similarly, Calderón-Chiu, Calderón-Santoyo, Herman-Lara, and Ragazzo-Sánchez (2021), obtained a jackfruit (*Artocarpus heterophyllus* L.) leaf protein hydrolysate by hydrolysis with pancreatin, which presented promising emulsifying properties. And in this context, it is suggested that the extract rich in pentacyclic triterpenes could be encapsulated by nanoemulsions stabilized with leaf protein hydrolysates. Hence, this protein hydrolysate could be considered an alternative to emulsifiers/encapsulants conventional of HVBC. To the best of our knowledge, the evidence published is not enough to demonstrate the possible application of leaf protein hydrolysate as wall material in emulsion formation. For that reason, additional studies on this subject are essential.

Therefore, the objective of this research was to optimize the conditions to obtain an optimal nanoemulsion (NE-Opt) loaded with triterpenic extract obtained from the leaf of *Coccoloba uvifera* L. and stabilized with the protein hydrolysate from jackfruit leaf. Then, the encapsulation efficiency and extract loading, the colour, and the stability of the NE-Opt were examined. Further, the NE-Opt was characterized by thermal gravimetric analysis (TGA) and differential scanning calorimetry (DSC).

Materials y methods

Materials

Jackfruit leaf was manually collected from the "Tierras Grandes" orchard located at Zacualpan, Compostela, Nayarit, Mexico (21° 15′N 105° 10′W), while the sea grape leaf was collected from the coast of Tecolutla, Veracruz, Mexico (20° 23′17″ N 97° 01′31″W). The leaves were washed and dried at 60 °C in a convective oven (Novatech, HS60-AID, Tlaquepaque, Jalisco, Mexico) for 24 h. Subsequently, they were ground, sieved (No. 100 mesh, 150 μm diameter), packed (vacuum-sealed bags), and stored at room temperature until use.

Chemicals

Pancreatin (EC 232-468-9) was acquired from Sigma-Aldrich (St. Louis, MO, USA). Sodium hydroxide (NaOH, PubChem CID: 14798) and hydrochloric acid (HCl, PubChem CID: 313) (reagent grade) were purchased from Thermo Fisher Scientific Inc., Waltham, MA, USA. Hexane (PubChem CID: 8058) and methanol (PubChem CID: 887) (reagent grade) were purchased from Jalmek® (Nuevo León, México). Extra virgin olive oil (Great value) was purchased from the local market.

Obtaining Coccoloba uvifera L. leaf extract

Coccoloba uvifera L leaf extract was obtained using the procedure described by Ramos-Hernández et al. (2018) whit modifications. The ground leaf was mixed with hexane in a 1:10 ratio. The mixture was placed in the ultrasonic bath (Digital Ultrasonic Cleaner, CD-4820, Guangdong, CHN) at 42 kHz for 30 min. Subsequently, the extract was filtered and the solvent was evaporated (RV 10 basic S1, IKA, Staufen, DEU). The concentrated extract (yield of 0.4%, Ramos-Hernández et al., 2018) was stored at room temperature until use.

Obtaining concentrate and protein hydrolysate from Artocarpus heterophyllus L. leaf

Extraction and hydrolysis of leaf protein concentrate (LPC) were carried out according to Calderón-Chiu et al. (2021). Briefly, the LPC of jackfruit was obtained with the isoelectric precipitation method and high hydrostatic pressure (HHP). For this, 30 g of jackfruit leaf were mixed with 563 mL of distilled water and 188 mL of 0.2 M NaOH. The mixture was treated in HHP (Isostatic press Flow Autoclave System, Avure Technologies AB, USA) at 300 MPa for 20 min (25 °C) and centrifuged at 15000*g* for 20 min (4 °C) (Hermle Z 326 K, Wehingen, DEU). The recovered supernatant was adjusted to pH 4.0 with 1 N HCl to precipitate the protein. The precipitated protein was recuperated by centrifugation (diafiltered with 1 kDa membrane), and lyophilized at −50 °C (0.12 mbar) in a freeze-drier (Labconco FreeZone 4.5, Kansas, MO, USA). Thus, LPC (yield of 32.00 ± 1.84%, Calderón-Chiu et al., 2021) was obtained. LPC hydrolysis was carried with pancreatin enzyme for 180 min. A solution of LPC (1%,w/v) was prepared with distilled water and incubated in a shaking bath (Shaking Hot Tubs 290200, Boekel Scientific, PA, USA) at 37 °C, 115 rpm. The solution was adjusted to pH 7.0 (1 N NaOH) and the enzyme was added in an enzyme-substrate ratio of 1:100 (w/w). The pH was maintained by adding NaOH if necessary. The enzyme was inactivated by heating the mixture at 95 °C (15 min) and adjusting pH to 7.0 and then centrifuged at 10000*g* for 15 min (4 °C). The supernatant was filtered (0.45 μm) and freeze-dried to obtain the pancreatin hydrolysate (H-Pan).

Solubility of the extract

The solubility of the triterpenic extract was determined by adding the extract (in excess) to 1 mL of soybean, sunflower, and olive oil. The samples were heated at 40 °C for 15 min. Then, they were kept under constant magnetic stirring for 48 h at 25 ± 1 °C. The samples were centrifuged (Hettich MIKRO 220R, Hettich, DEU) at 18840*g* for 30 min (15 °C) to remove excess undissolved extract and the supernatant was recovered (Fasolo et al., 2020). The supernatant was filtered (0.45 μm) and adequately diluted with methanol for the determination of the extract content at 210 nm using a spectrophotometer (Cary 50 Bio UV–Visible, Varian, Mulgrave, AUS). The content of triterpenic extract was expressed as equivalents of lupeol, one of the major components of the extract (Ramos-Hernández et al., 2018). A calibration curve of lupeol (dissolved in methanol) ranging from 0 to 1000 ug/mL was performed and calculation was done using the straight line equation, $y = 0.9699x - 0.0036$; $R^2 = 0.9978$.

Box–Behnken design for optimization of nanoemulsion

The NE-Opt was optimized through a Box-Behnken design (BBD). The design employed three-factor, low (−1), medium (0), and high (+1), the range of independent variables was chosen based on the result of various initial trials. The independent variables were protein hydroly-

sate (X_1), oil loaded with extract (X_2), and ultrasound time (X_3), while polydispersity index (PDI, Y_1), surface-weighted mean diameter (D[3,2], Y_2), and volume-weighted mean particle diameter (D[4,3], Y_3) constituted the dependent variables (Table S1, Supplementary material). The design presented 15 experimental runs (Table 1) and the quadratic model is shown in the Equation. (1):

$$Y = b_0 + b_1X_1 + b_2X_2 + b_3X_3 + b_{12}X_1X_2 + b_{13}X_1X_3 + b_{23}X_2X_3 + b_{11}X_1^2 + b_{22}X_2^2 + b_{33}X_3^2 \quad (1)$$

where Y is the predicted response(s); b_0 is the intercept; b_1, b_2, b_3 are linear coefficients; b_{12}, b_{13}, b_{23} are the interaction coefficients; b_{11}, b_{22}, b_{33} are the square coefficients; and X_1, X_2, and X_3 are the independent variables. Response surface methodology (RSM) was performed using Statistica software version 10.0 (StatSoft, Inc., 2011). Responses were statistically evaluated by ANOVA. Optimal conditions (NE-Opt formulation) were obtained using the desirability function.

Preparation of emulsions

Emulsions were prepared according to described by Miss-Zacarías, Iñiguez-Moreno, Calderón-Santoyo, and Ragazzo-Sánchez (2020) with modifications. The aqueous phase was prepared by dissolving the H-Pan in distilled water. The pH of the solution was adjusted to 8.0 and kept under magnetic stirring (700 rpm) for 24 h at room temperature. Then, the solution was centrifuged (Hermle Z, 326 K, Wehingen, DEU) at 2350*g* for 30 min (20 °C). The oil with the highest amount of dissolved extract constituted the oil phase. Subsequently, the oily phase was gradually added to the solution of H-pan (aqueous phase) with agitation (IKA T10 basic ultra turrax, Staufen, DEU) at 10,000 rpm for 5 min to homogenize both phases. This preemulsión was processed by Digital Sonifier® Unit, model S-150D (Branson Ultrasonics Corporation, Danbury, CT, USA) at 24 kHz.

Particle size distribution of emulsions

The emulsion particle size distribution was measured by Mastersizer 3000 Hydro EV (Malvern, Worcestershire, UK). Measurements were performed at 25 °C and the refractive index was set as 1.46 for dispersed phase (olive oil) and 1.33 for dispersant (water). Briefly, 400 mL distilled water was placed in the Hydro EV unit. Then, the emulsion was added dropwise until a laser obscuration of 8–12% was obtained. The emulsions were analysed five successive times in the diffractometer and a mean size distribution curve was obtained. The particle size of the emulsions was represented as PDI, D[3,2], and D[4,3]. These parameters were obtained from the full particle size distribution and calculated automatically using the Mastersizer 3000 software version 3.60 (Worcestershire, UK).

Encapsulation efficiency and extract loading

Encapsulation efficiency (EE%) and drug loading (DL%) of the NE-Opt were carried out with the methodology of Kalam, Khan, Khan, Almalik, and Alshamsan (2016), with modifications. The EE% and DL% were determined by calculating the content of free extract in the dispersion medium. Briefly, 1 mL of nanoemulsion was added to a 2 mL centrifuge tube and centrifuged at 18840*g* for 15 min (15 °C). After centrifugation, there were two layers: an aqueous phase at the bottom (free extract) and a thin protein layer on the aqueous phase (encapsulated extract). The solution at the bottom was carefully collected and placed in another centrifuge tube. Subsequently, 1 mL of chloroform: acetone solution (1:1; v/v) was added to the tube and vortexed for one min. After, the solution was centrifuged (Hettich MIKRO 220R, Hettich, DEU) at 18840*g* for 30 min (15 °C). The organic phase at the bottom was carefully collected, filtered (0.45 μm), and diluted with methanol for the determination of extract free using a spectrophotometer at 210 nm as mentioned above in section 2.5. The EE% and LD% were calculated (Eqs. (2) and (3)).

$$EE = \frac{Initialamountofextract - Freeextract}{Initialamountofextract} x100 \quad (2)$$

$$LD = \frac{Initialamountofextract - Freeextract}{Amountoflipidused} x100 \quad (3)$$

Emulsion stability index

The emulsion stability index (ESI) was calculated as described by Calderón-Chiu et al. (2021). A 50 μL sample of the NE-Opt was diluted 100-fold whit a 0.1% SDS solution. The diluted sample was vortexed (10 s) and the absorbance was read at time 0 (A_0) and 10 min (A_{10}) after emulsion formation in a spectrophotometer (Cary 50 Bio UV–Visible, Varian, Mulgrave, AUS) at 500 nm. Then, the emulsion stability index was calculated (Eq. (4)).

Table 1
Box–Behnken design with experimental and predicted values of PDI, D[3,2] and D[4,3].

Formulations	Independent variables			Dependent variables					
				Experimental response			Predicted response		
	X_1	X_2	X_3	Y_1	Y_2	Y_3	Y_1	Y_2	Y_3
F1	0.50	2.5	10	1.08 ± 0.06	0.44 ± 0.00	0.51 ± 0.01	1.08	0.44	0.51
F2	2.00	2.5	10	0.95 ± 0.07	0.45 ± 0.04	0.51 ± 0.06	0.95	0.45	0.5
F3	0.50	7.5	10	2.20 ± 0.06	1.42 ± 0.07	2.46 ± 0.15	2.20	1.42	2.46
F4	2.00	7.5	10	1.03 ± 0.00	0.37 ± 0.00	0.42 ± 0.00	1.03	0.37	0.42
F5	0.50	5.0	5	1.85 ± 0.06	0.96 ± 0.09	1.43 ± 0.13	1.85	0.96	1.42
F6	2.00	5.0	5	1.23 ± 0.00	0.58 ± 0.00	0.73 ± 0.02	1.22	0.58	0.73
F7	0.50	5.0	15	2.33 ± 0.38	0.68 ± 0.06	1.01 ± 0.12	2.33	0.68	1.01
F8	2.00	5.0	15	1.05 ± 0.02	0.45 ± 0.00	0.52 ± 0.00	1.05	0.45	0.52
F9	1.25	2.5	5	1.37 ± 0.19	0.64 ± 0.04	0.83 ± 0.10	1.36	0.64	0.83
F10	1.25	7.5	5	2.36 ± 0.07	0.82 ± 0.01	1.28 ± 0.04	2.36	0.82	1.28
F11	1.25	2.5	15	0.86 ± 0.03	0.35 ± 0.04	0.38 ± 0.04	0.86	0.35	0.38
F12	1.25	7.5	15	3.15 ± 0.00	0.66 ± 0.00	1.15 ± 0.01	3.15	0.66	1.14
F13	1.25	5.0	10	3.69 ± 0.28	0.58 ± 0.06	1.01 ± 0.12	3.66	0.56	0.97
F14	1.25	5.0	10	3.55 ± 0.11	0.57 ± 0.07	0.97 ± 0.16	3.66	0.56	0.97
F15	1.25	5.0	10	3.75 ± 0.17	0.54 ± 0.01	0.93 ± 0.00	3.66	0.56	0.97
NE-Opt	**1.25**	**2.5**	**15**	**0.85 ± 0.02**[a]	**0.33 ± 0.03**[a]	**0.36 ± 0.03**[a]	**0.86**[b]	**0.35**[b]	**0.37**[b]

X_1 = Protein hydrolysate (%), X_2 = Oil loaded with extract (%), X_3 = Ultrasound time (min), Y_1 = PDI, Y_2 = D[3,2] (μm), Y_3 = D[4,3] (μm), NE-Opt = Optimal nanoemulsion.

$$ESI = \frac{A_0}{A_0 - A_{10}} x t \quad (4)$$

where t is the time interval (10 min). The ESI of the emulsion was expressed in min.

Stability of the emulsion

Storage stability

Freshly produced NE-Opt (10 mL) was placed in vials glass and kept in a vertical position at 4 and 25 ± 1 °C for 0, 1, 15, and 30 days. ESI of the NE at different days of storage was evaluated (Ruiz-Montañez, Ragazzo-Sanchez, Picart-Palmade, Calderón-Santoyo, & Chevalier-Lucia, 2017).

pH stability

Freshly produced NE-Opt (10 mL) was placed in 20 mL beakers. Then, the NE-Opt was adjusted to different pH values (2.0–8.0) with 1 N HCl or NaOH. The emulsion was vortexed and placed in vials glass (Zang et al., 2019). ESI of NE was measured after storage for 24 h at 25 °C.

Temperature stability

Freshly produced NE-Opt (10 mL) was transferred to vial glass, which was placed into a convective drying oven at temperatures of 30–90 °C for 30 min, followed by cooling to room temperature (Xu et al., 2016). The NE was vortexed and the ESI was measured after storage for 24 h at 25 °C.

Ionic strength stability

Freshly produced NE-Opt (10 mL) was transferred into vial glass. Then, different amounts of 1 M NaCl solution were added to the NE-Opt to obtain emulsions with final salt concentrations of 100 to 500 mM (Ozturk, Argin, Ozilgen, & McClements, 2015). The NE was vortexed and the ESI was measured after storage for 24 h at 25 °C.

Colour of the emulsion

The colour of the NE-Opt with and without extract was measured with a MINOLTA Chroma Meter CR-400 (Minolta Co. Ltd. Osaka, JPN) (Calderón-Chiu et al., 2021). The colorimeter was calibrated with white tile (L^*= 95.13, a^*= −0.94, and b^*= 2.93) before the measurement. The colour was recorded as lightness (L^*), redness (a^*, ±red-green), and yellowness (b^*, ±yellow-blue). The NE-Opt with extract was stored at 25 and 4 °C for 30 days to evaluate the colour changes in storage and the total colour difference (ΔE) was calculated on the different days (Equation (5)).

$$\Delta E = \sqrt{\left(L^* - L_0^*\right)^2 + \left(a^* - a_0^*\right)^2 + \left(b^* - b_0^*\right)^2} \quad (5)$$

where ΔE is the total colour difference; L_0^*, a_0^*, b_0^* are the colour parameters at day 0; L^*, a^*, b^* are the colour parameters at 15 and 30 days of storage.

Thermal properties of the emulsion

Thermal analyses were performed on each emulsion component (H-Pan and olive oil), as well as the NE-Opt with and without extract (Miss-Zacarías et al., 2020). Thermogravimetric analysis (TGA) was done using TGA 550 equipment (TA Instruments, New Castle, USA). The sample (5–10 mg) was heated from 25 to 800 °C with a heating rate of 10 °C/min under a nitrogen flow. The differential scanning calorimetry (DSC) was achieved using DSC 250 equipment (TA Instruments, New Castle, USA). The samples (3–4 mg) were hermetically sealed in aluminium pans and heated from 25 to 250 °C at a heating rate of 10 °C/min under nitrogen flow with an empty pan as a reference. The samples were analysed in triplicate and the thermograms obtained were analysed by the software TRIOS 5.0.0.44616.

Statistical analysis

Results from the solubility of extract in oil and ESI of NEs (n = 3) were achieved with a one-way analysis of variance (ANOVA). Then post-hoc by LSD (least significant difference) was performed for the mean comparison ($P < 0.05$) with the Statistica software version 10.0 (StatSoft, Inc., 2011). RSM was realized to determine the optimum conditions of the independent variables on desired responses.

Results and discussion

Solubility of the extract in the oil

The ability of lipid nanostructures to encapsulate a compound depends on its solubility in the lipid phase. Thus, the solubility of extract in olive (74.23 ± 0.59), soybean (67.85 ± 1.66), and sunflower oil (67.39 ± 0.87) was determined. The effectiveness of olive oil is attributed to its composition of fatty acids that affect the co-solvency properties. Olive oil has a higher composition of mono- and diacylglycerols than soybean and sunflower oil. Mono- and diacylglycerols are amphiphilic (surface-active), for this reason, they are the most widely used emulsifiers in the food industry (Balata, Eassa, Shamrool, Zidan, & Abdo Rehab, 2016). Therefore, olive oil was chosen as the oil phase for the formulation of nanoemulsions. Additionally, this oil has high oxidative stability, great nutritional value, and a fatty acid profile that is beneficial for human health (Ambrosone, Cinelli, Mosca, & Ceglie, 2006).

Fitting the models

The effects of protein hydrolysate concentration, oil concentration (with extract), and ultrasound time were investigated to find a NE-Opt loaded with extract rich in pentacyclic triterpenes. The BBD produced 15 different formulations, the responses experimental and predicted are shown in Table 1. ANOVA and the coefficients of determinations (R^2 and adjusted R^2) of PDI, D[3,2], and D[4,3] are shown in Table S2 (Supplementary material). The regression analysis shows that the R^2 for responses Y_1, Y_2, and Y_3 was 0.9887, 0.9857, and 0.9850, respectively. In a correctly fitted model, R^2 should be>0.8. Therefore, the R^2 values obtained indicate that the models adequately described the relationship between the independent variables evaluated and that>90% of the experimental responses can be explained by the model, which is considered a robust model. On the other hand, the adjusted R^2 of Y_1, Y_2, and Y_3 were 0.9807, 0.9757, and 0.9744, respectively. These values are very close to the R^2 values, which indicates a good correlation between the experimental and predicted values.

Effect of protein hydrolysate concentration, oil concentration, and ultrasound time on PDI

The uniformity of the particles in a NE produces a homogeneous mixture with a narrow size distribution, which is an essential prerequisite for nanoemulsions. The variables with the largest effects on PDI were the quadratic effect of protein hydrolysate concentration, oil concentration, and ultrasound time. Whereas, the lineal effect of ultrasound time had no impact ($P > 0.05$) on the PDI of nanoemulsions (Table S2, Supplementary material). The positive coefficients of X_1 and X_2 in the model for PDI (Equation 6, Table S2, Supplementary material) indicate that there would be an increase in PDI with the increase in protein hydrolysate and oil concentration. The model indicates that a low concentration of these variables leads to a decrease of PDI of NEs (Aqil, Kamran, Ahad, & Imam, 2016).

Effect of protein hydrolysate concentration, oil concentration, and ultrasound time on D[3,2]

The variables with the largest effects on the D[3,2] were the linear

effect of protein hydrolysate concentration, the interaction between protein hydrolysate and oil concentration, and the lineal effect of oil concentration. Since the quadratic effect of oil concentration and ultrasound time did not show any influence on the D[3,2] of the NEs ($P > 0.05$), they were not included in the final model. The quadratic model for D[3,2] (Equation 7, Table S2, Supplementary material) shows a positive coefficient for X_1, which indicate the increase in D[3,2] with the increment of protein hydrolysate concentration, whereas the negative value of X_2 and X_3 indicates a decrease in D[3,2] with an increasing oil concentration and ultrasound time. This model suggests that reducing the protein hydrolysate concentration and increasing the oil concentration and ultrasound times can decrease the D[3,2]. The presence of high emulsifier concentration increases the apparent viscosity of the prepared emulsions. This decreases the efficiency of ultrasound emulsification, leading to higher coalescence rates, which results in larger droplet sizes (Tang, Manickam, Wei, & Nashiru, 2012).

Effect of protein hydrolysate concentration, oil concentration, and ultrasound time on D[4,3]

For D[4,3], the variables with the largest effects were the linear effect of protein hydrolysate concentration and oil concentration, followed by the interaction between protein hydrolysate concentration and oil concentration (Table S2, Supplementary material). The quadratic effect of ultrasound time, the interaction between protein hydrolysate and oil concentration, and the quadratic effect of protein hydrolysate and oil concentration had no significant effects ($P > 0.05$), then, these terms were not included in the final model. The quadratic model for D[4,3] (Equation 8, Table S2, Supplementary material) shows a positive coefficient for X_1 and X_2, which indicates the increase in D[4,3] values with the increment of concentration of protein hydrolysate and oil. The negative coefficient X_3 shows the decrease in D[4,3] with an increase in ultrasound time. Therefore, the model suggests that a low concentration of protein hydrolysate and oil with the increase in the ultrasound time could decrease D[4,3] values. With the high oil concentrations, the disruption process of droplets is more difficult due to the high viscosity in the dispersed phase. This causes greater resistance to flow, whereby the rate of breaking of the droplet is severely restricted. The increases in the viscosity of the oil phase result in emulsions with larger particle size distribution (Tang et al., 2012).

Response surfaces analysis

The effects of protein hydrolysate, oil loaded with extract, and ultrasound time on PDI, D[3,2], and D[4,3] are shown in the desirability surfaces plot (Fig. 1), which are useful to analyse the effects of two factors on the response at the same time (Aqil et al., 2016). Whereas the linear correlation plots between experimental and predicted values of PDI, D[3,2], and D[4,3] are shown in Fig. 2A, 2B, and 2C, respectively. The effect of the concentration of protein hydrolysate and oil loaded with extract on the desirability of the three responses evaluated (Fig. 1A) indicated that increasing oil decreases the desirability of the responses. Therefore, the average droplet size and PDI increases as the oil content increases. This caused the aggregation of particles because the amount of protein hydrolysate was not sufficient to create a protective layer on each particle. Since at low concentration of emulsifier and high oil content, the emulsifier es not enough to completely cover the newly formed oil–water interface, and this limitation of the emulsifier

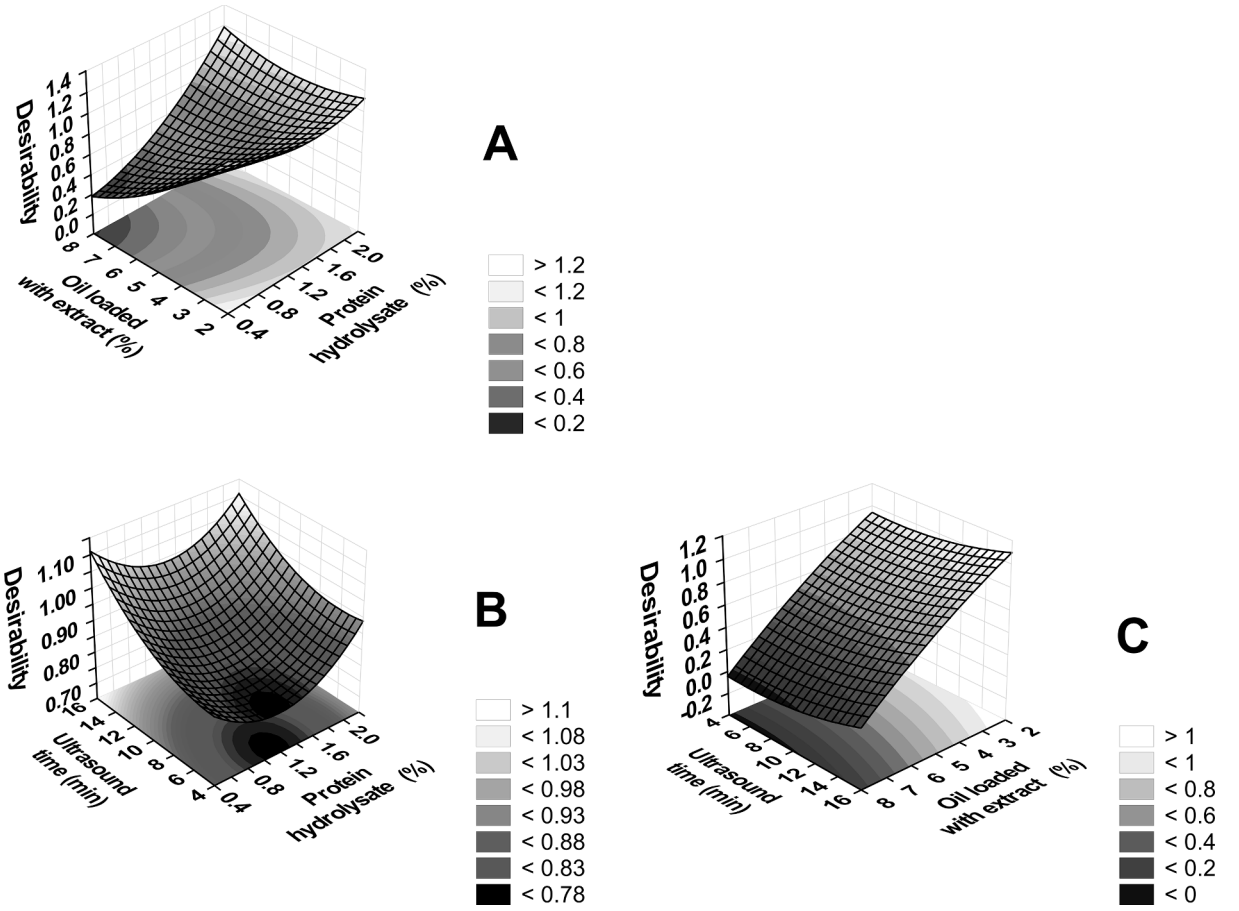

Fig. 1. Desirability surface plots of the interactions between oil loaded with extract-protein hydrolysate (A), ultrasound time-protein hydrolysate (B), and ultrasound time-oil loaded with extract (C).

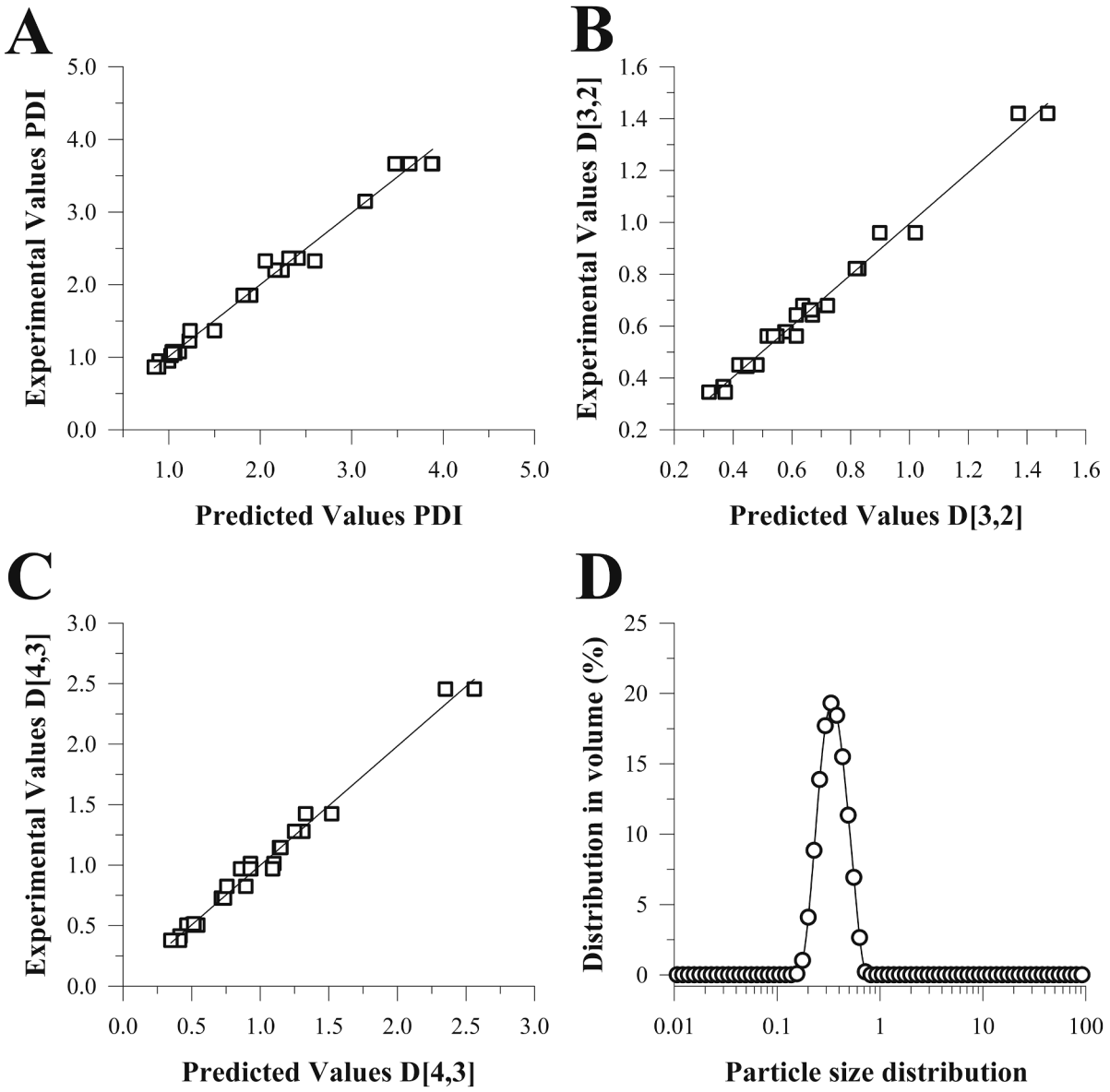

Fig. 2. Linear correlation plots between experimental and predicted values of PDI (A), D[3,2] (B), and D[4,3] (C) and particle size distribution (D) of the NE-Opt.

increases the droplet size (Kentish et al., 2008). However, an increase in desirability was observed when the protein hydrolysate concentration was increased. This agrees with the findings of Yasir and Sara (2013).

Concerning the effects of ultrasound time and protein hydrolysate concentration on the desirability of the responses evaluated, increasing the sonication time tended to increases the desirability of responses (Fig. 1B). This suggests the decrease in the droplet size distribution, caused by the increase in the sonication time, which allowed the intensification of the shear forces (during the acoustic cavitation) and facilitated the breaking of large droplets. Moreover, a longer sonication time increases the solubility and the rate of adsorption of protein hydrolysate at the interface; increasing the amount of protein adsorbed at the oil interface improves emulsion stability (Taha et al., 2020). These results are consistent with the findings by Pongsumpun, Iwamoto, and Siripatrawan (2020), who reported that the particle size of cinnamon essential oil nanoemulsions decreases whit increasing ultrasound time.

Fig. 1C shows the effects of ultrasound time and oil loaded with extract on the desirability of the responses evaluated. The increase in the oil concentration decreased the desirability of the evaluated responses, which suggests an increase in particle size distribution. This can be attributed to the fact that an increase in the oil content makes the droplet breaking process difficult during sonication due to the increased resistance to the flow (Tang et al., 2012). However, an increase in desirability was observed with decrease oil concentration and the increase in ultrasound time. This promoted a successful coating of the dispersed droplets and reduced the interfacial tension between the oily and aqueous phases.

Validation and verification of the predicted optimal conditions

The NE-Opt, which should have the lowest value of PDI, D[3,2] and D[4,3] was obtained using the desirability function (value of 0.99). The PDI, D[3,2] and D[4,3] were optimized at 0.86, 0.35 μm, and 0.37 μm, respectively. These optimal values could be achieved with 1.25% protein hydrolysate, 2.5% oil loaded with extract, and 15 min of ultrasound (Table 1). For validation, additional experiments (triplicate) were performed using the optimized parameters. The experimental results were significantly different ($P < 0.05$) from the data obtained from desirability optimization analysis. However, the experimental results of PDI (0.85 ± 0.02), D[3,2] (0.33 ± 0.03 μm) and D[4,3] (0.36 ± 0.03 μm)

(Table 1) for the NE-Opt are very close to those predicted by the models. Then, the results suggested the model was satisfactory and accurate. Additionally, PDI measures the homogeneity of particles in a sample and ranges from 0 to 1. If the PDI value is closer to zero, it indicates higher homology between the particles of a sample (Aslam et al., 2016). The experimental PDI value was significantly lower than predicted and it is in the acceptable range. Furthermore, the NE-Opt showed a particle size distribution in the nanometric range and monomodal distribution (Fig. 2D), which is indicative of a homogeneous and stable emulsion.

Encapsulation efficiency and extract loading

The EE% and LD% of the NE-Opt were 40.15 ± 1.46 and 18.03 ± 2.78% respectively. The low EE% and LD% values of NE-Opt could be attributed to the low proportions of oil and H-Pan used for its preparation since EE% and LD% depend on the solubility of the drug in the oil phase and the partition of the drug between the oily and aqueous phase (Aslam et al., 2016). However, our results were very close to those reported by Yasir and Sara (2013), who observed an increase in EE% and LD% on increasing the drug lipid ratio. On the other hand, H-Pan also role in the encapsulation of the core of emulsion. Encapsulation properties of protein-stabilized emulsions have been studied as a function of the different core to wall ratios. Higher EE% has been noted at a low core to wall ratio. Then, it should be noted that low concentrations of H-Pan can encapsulate up to 40% oil with extract, which could show the good encapsulating properties of H-Pan. Though, an increase in EE% and LD% might be achieved by combining H-Pan with maltodextrin (protein-carbohydrate), which is a better method to reach an efficient encapsulation (Galves, Galli, Miranda, & Kurozawa, 2021).

Stability of the emulsion

Storage stability

ESI measures the resistance of the emulsion over a specific time and was used to measure the stability of the NE-Opt under different conditions. The changes in the ESI of NE-Opt were measured during 30 days of storage at 4 and 25 °C (Fig. 3A). The initial ESI of the NE-Opt was 108.15 ± 12.1(day 0) and decreased significantly ($P < 0.05$) throughout the storage period to 47.62 ± 4.97 and 66.12 ± 12.33 for NEs storage at 4 and 25 °C, respectively. The decrease in ESI could be indicative of an increase in the particle size distribution of NEs throughout the storage period. This increase in particle size in the NEs has been associated with

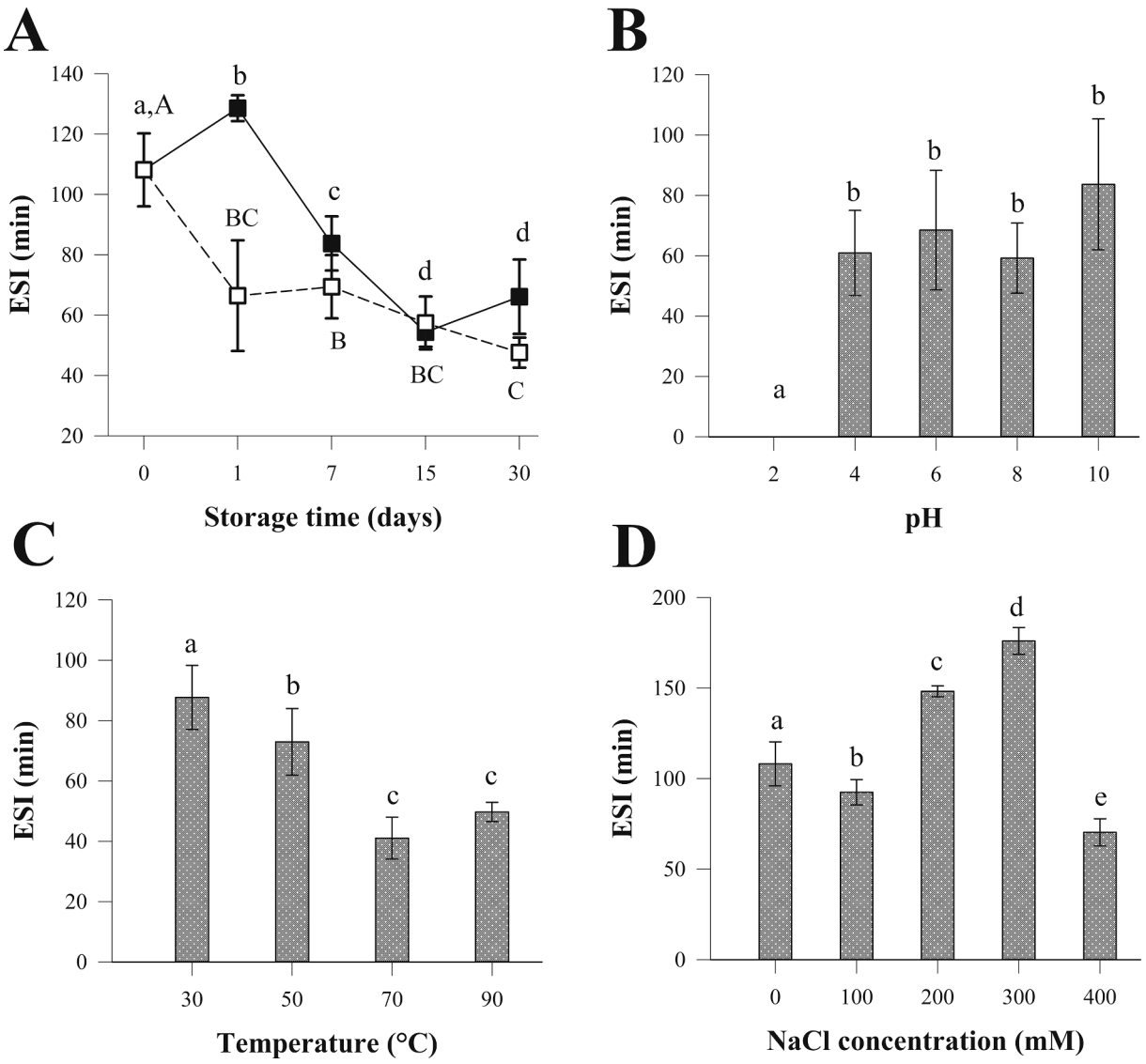

Fig. 3. Emulsion stability index (ESI) of NE-Opt during the storage [4 (□) and 25(■) °C] (A), pH (B), temperature (C), and NaCl concentration (D). Different letters indicate significant differences ($P < 0.05$) between treatments. Lines are for the guidance of reader.

droplet flocculation (Ling et al., 2020). The decrease in NEs stability due to increased particle size could be produced by changes in the protein conformation. During aging, proteins form non-covalent bonds (e.g., hydrogen and hydrophobic) with neighboring proteins at the interface. The formation of intermolecular bonds between the adsorbed protein molecules transforms the adsorption layer into a fragile/brittle shell, which ruptures upon surface expansion and deformation, and causes the stability of the emulsion to decrease (Lam & Nickerson, 2013).

In NEs stored at 25 °C, ESI decreased significantly ($P < 0.05$) during days 1, 7, and 15 of storage. Nevertheless, the extension of the storage period to 30 days had no significant effect ($P > 0.05$) in the ESI. Concerning NE stored at 4 °C, there were no significant differences in ESI during days 1, 7, and 15 of storage. But, after 30 days of storage, a significant decrease in ESI was observed. The decrease in ESI was relatively more pronounced in NEs stored at 4 °C. This is due to a phenomenon known as partial coalescence, which occurs when O/W emulsions are chilled to temperatures where the oil phase partially crystallizes while the aqueous phase remains liquid. Then, the globules do not coalesce into one drop, although there is oil–oil contact between them (McClements, 2004). Then, the emulsifier is adsorbed on the surface of ice crystals, reducing the number of emulsifiers to cover the emulsion droplets. Nonetheless, there were no significant differences ($P > 0.05$) in ESI between the emulsions stored at 4 and 25 °C during the 7, 15, and 30 days of storage, which indicates that NEs have a similar behaviour at both temperatures.

Influence of pH

The influence of pH on the ESI of NE-Opt was examined (Fig. 3B). The ESI of the NE-Opt decreased significantly ($P < 0.05$) in all tested pHs, and its decrease could indicate an increase in particle size distribution. NE-Opt showed greater instability at pH 2.0, resulting in oil and water phase separation in the system. This behaviour was described by Zang et al. (2019) in O/W emulsions stabilized with rice protein hydrolysate. They indicated that emulsions with a pH at or near the isoelectric point (pI) cause surface neutrality, since the number of positively charged groups (amino) is equal to the number of negatively charged groups (carboxyl) on the interface O/W. Therefore, the net charge of the droplet was too low to avoid van der Waals attraction near the pI. This lead to an increase in droplet size as a result of droplet aggregation, which caused a greater degree of instability (Ozturk et al., 2015).

In contrast, from pH 4.0 to 10.0, the NEs were relatively more stable and there were no significant changes ($P > 0.05$) in ESI with increasing pH. This phenomenon may be due to the increased negative charge of the carboxyl group and the neutrality of the amino group, which makes the droplets have a net negative charge (Zang et al., 2019). Hence, the stabilization mechanism that avoids droplet aggregation in NE stabilized with H-Pan is electrostatic repulsion. This trend is similar to that reported by Sarkar, Kamaruddin, Bentley, and Wang (2016) in emulsions stabilized by tomato seed protein isolate. The results suggest that H-Pan has potential as an emulsifier and could be used to formulate an emulsion under conditions of pH conditions of 4.0–10.0.

Influence of temperature

Temperature conditions influence the stability of food products containing protein-coated lipid droplets (Sarkar et al., 2016; Zang et al., 2019). Thus, it is imperative to explore the effect of heating on the stability of NE-Opt. Heat treatment at 30–70 °C of the NE-Opt had a significant ($P < 0.05$) influence on the ESI (Fig. 3C). The thermal treatments reduced the ESI of the NE-Opt from 87.67 ± 10.64 min (30 °C) to 49.71 ± 3.18 min (90 °C), which could indicate an increase in droplet size as a function of temperature. The apparent increase in the droplet size of NE-Opt could be the result of heat-induced droplet aggregation. This led to changes in the conformation of the adsorbed proteins at the O/W interface from 70 °C, which reduced the electrostatic repulsion or a structural change in non-polar or sulfhydryl groups as was reported by Pan et al. (2019) in rice protein hydrolysate stabilized emulsions. Then, the results suggest that heating altered the number or location of the charged groups at the droplet surfaces (Xu et al., 2016).

Influence of ionic strength

The effect of NaCl on the stability of NE-Opt is shown in Fig. 4D. The ESI of NE-Opt prepared with H-Pan showed a significant increase in ESI with increment NaCl concentration from 0 mM (108.15 ± 12.1 min) to 300 mM (176.05 ± 7.41 min); however, the increase in the concentration to 400 mM decreased the ESI drastically (70.3 ± 7.49 min). This indicates that the NE-Opt was stable to aggregation in presence of ≤ 300 mM NaCl. The improvement in the ESI of NE-Opt could be because the increase in the concentration of NaCl produced changes in the solubility of H-Pan. At high pH values, proteins show an increased negative charge that, combined with the salting-in effect of NaCl, dissociates the protein aggregates and rises the solubility. The higher solubility increases the availability of soluble proteins that can be absorbed in the interface. This contributes to greater electrostatic repulsion between droplets and decreases their flocculation (Fernández Sosa, Chaves, Henao Ossa, Quiroga, & Avanza, 2021).

Nevertheless, when the NaCl concentration was increased at 400 mM, the electrostatic repulsion was not sufficient to overcome the interactions of attraction between the emulsion droplets, causing aggregation and instability of NE due to electrostatic screening and ion-binding effects (McClements, 2004). In the electrostatic screening effect, the accumulation of monovalent ions (Na^+, opposite charge) on the surface of the oil globules, neutralizes the charge in the emulsion droplets and inactive the electrostatic barrier that protects the emulsion droplet from globule-globule interactions (Drapala, Mulvihill, & O'Mahony, 2018). This behaviour is similar to that reported in emulsions-stabilized by rice protein hydrolysates (Xu et al., 2016; Zang et al., 2019). However, it should be noted that the NE-Opt stabilized with H-Pan showed stability to high concentrations of NaCl (300 mM) since an improvement in the ESI was observed. In contrast, the emulsions mentioned above were unstable from 100 mM NaCl. This showed that the NE-Opt was relatively stable to aggregation induced by monovalent ions.

Colour of the emulsion

The evaluation of colour changes during storage is important for consumer acceptance, maintaining the original colour in food emulsions is a key point. The values of L^* (45.14 ± 2.27), a^* (8.06 ± 0.25), and b^* (10.93 ± 0.46) of the NE-Opt without extract (control) were significantly different ($P < 0.05$) whit the NE-Opt with extract. The NE-Opt with extract showed lower values of L^* (40.50 ± 1.75) and a^* (3.96 ± 0.21) with respect to NE control, while an increase in b^* (13.17 ± 0.70) was observed. These differences could be associated with the incorporation of the triterpenic extract. The sea grape leaf extract presents low values of L^* (19.85 ± 1.3), a^* (-0.18 ± 0.14), and b^* (00.14 ± 0.16), which when combined with the other components of the NE, caused the decrease in brightness and a slight increase in greenness. This green colour is a visual characteristic of the triterpenic extract.

Regarding the days of storage, the NE-Opt with extract presented a significant increase ($P < 0.05$) in L^*, a^*, and b^* after 15 days of storage (Fig. 4). And the extension of the storage time to 30 days did not cause significant changes ($P > 0.05$) in these colour parameters both in emulsions stored at 25 and 4 °C. In this sense, Silva et al. (2011) reported a similar trend in nanoemulsions of β-carotene. They observed that the L^* parameter increased during 21 days of storage. As for the effect of temperature, there were no significant differences ($P > 0.05$) in the colour parameters between the emulsions stored at 25 and 4 °C at 15 days, while at day 30 significant differences ($P < 0.05$) were observed in a^* and b^* between the emulsions stored at 25 and 4 °C (Fig. 4B and Fig. 4C). The parameter a^* was higher in the NE stored at 4 °C, which indicates the decrease in the greenness at low temperature. Conversely,

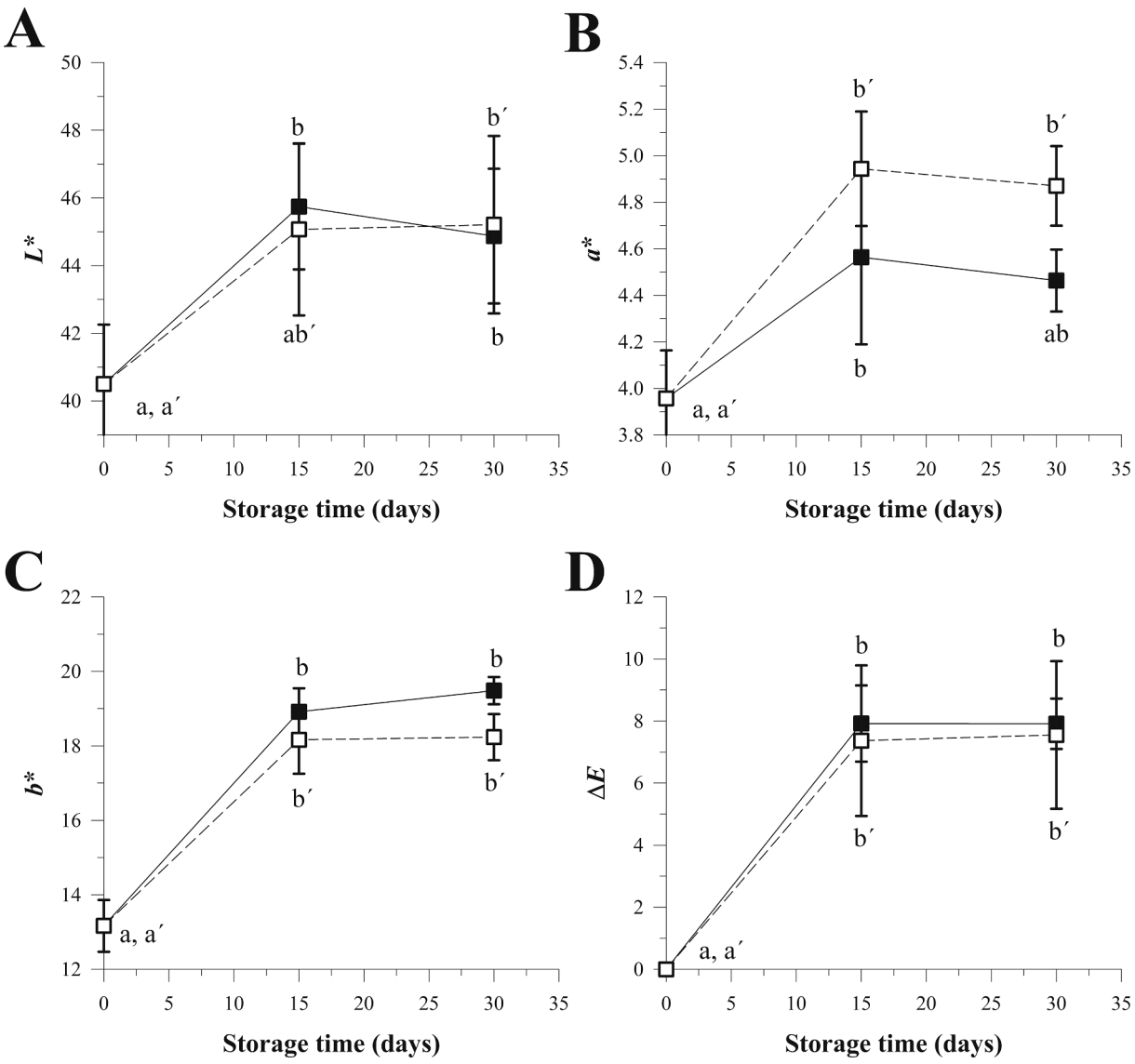

Fig. 4. Evolution of the NE-Opt color parameters during storage at 25 (■) and 4 (□) °C: A) L*: Lightness; B) a*: redness; C) b*: yellowness and D) ΔE: Total color difference. [a–b or á–b́]indicate significant differences ($P < 0.05$) between emulsions stored at 0, 15, and 30 days for temperatures of 25 and 4 °C, respectively. Lines are for the guidance of readers.

*b** was lower in the NE stored at 4 °C, indicating the reduction in the yellowness of the NE. The high values of *a** could be associated with the low stability of the emulsions stored at 4 °C as shown previously in section 3.6.1. The emulsions stored at 4 °C were apparently more unstable due to the partial crystallization of the oil with encapsulated extract, which caused a possible increase in *a**.

Finally, the total colour difference (Δ*E*) presented a similar trend to the parameters *L**, *a**, and *b**. Fig. 4D shows that there was a significant increase ($P < 0.05$) in the Δ*E* of the NE-Opt after 15 days of storage, while at day 30 no significant differences were observed in Δ*E* comparing with the reference values (day 0). The results showed that both the Δ*E* (Fig. 4D) and ESI (Fig. 3A) of the NE-Opt have similar behaviour in the storage since after 15 days no significant changes were observed. This could indicate that the changes in the colour of nanoemulsions depend on emulsion stability. Then, the changes in Δ*E* during storage might be due to changes in particle size distribution that lead to changes in the colour parameters of nanoemulsions (Silva et al., 2011). Our results confirm those previously described by Silva et al. (2011) and Saravana et al. (2019), who indicated that colour measurement is a complementary method for evaluating the stability of NEs.

Thermal properties of the emulsion

The TGA patterns of the NE-Opt and its components are shown in Fig. 5A. The TGA thermogram shows that H-Pan presented three stages of weight loss. The first weight loss (about 6.31%) from 34.82 to 46.66 °C belongs to water evaporation. The second (40.66%) and third (42.75%) weight losses occurred at 220.0–327.12 °C and 453.36–604.83 °C, respectively. These weight losses could be associated with the volatilization of protein fragments with different molecular weights that are generated by enzymatic hydrolysis of LPC, which have different thermal stability (Personal communication). The triterpenic extract presented two weight losses which are mainly related to the decomposition of extract components. The first weight loss occurred at 218.45–281.48 °C (65.96%). These decomposition temperatures are comparable to those described by da Silva-Júnior and de Pinheiro (2017) and Vieira-Júnior, de Souza, and Chaves (2005), which were related to the volatilization of the mixture of α, β amyrin. The second loss occurred at 326.84–371.88 (28.95%) and could be associated with the decomposition of betulina (350 °C) or betulinic acid (370 °C) (Anghel et al., 2013), which are derived from the oxidation of lupeol.

The NE-Opt without and with extract showed two weight losses. TGA

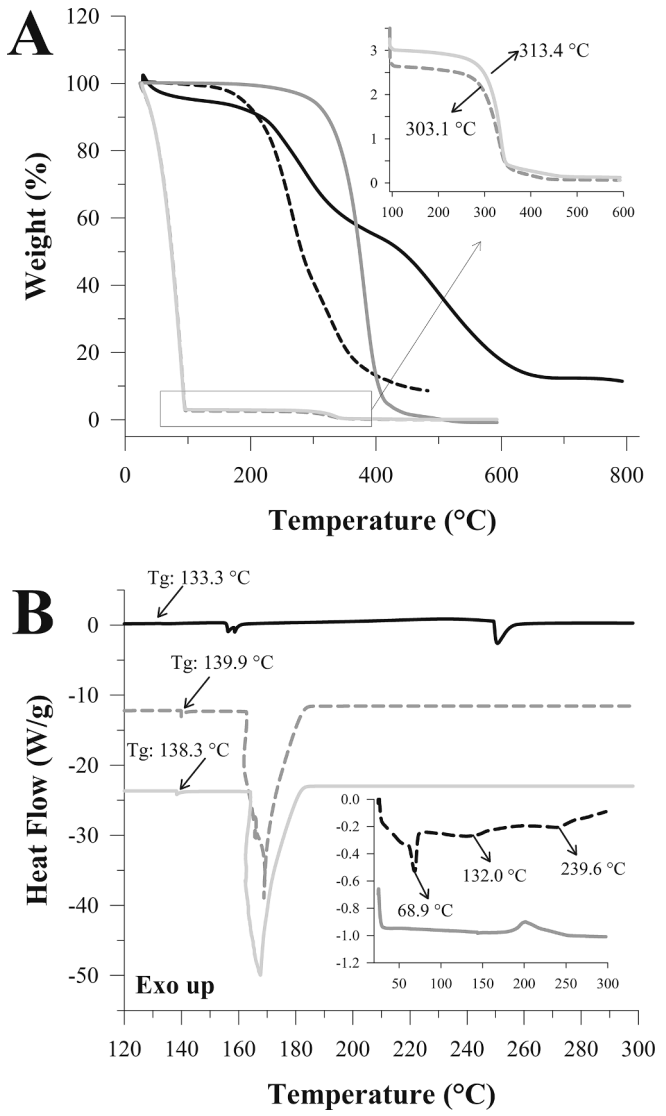

Fig. 5. Thermal analysis of emulsion and its components: A) DSC and B) TGA of H-pan (), triterpenic extract (), oil olive (), NE-Opt without extract () and with extract ().

thermogram indicated that the first weight loss for NE without (96.27%) and with extract (95.88%) occurred in the range of 66.71–95.28 °C and 66.16–94.75 °C, respectively. These weight losses are due to the loss of water from the surface of the emulsion (Saravana et al., 2019). The second loss for NE without and with extract arisen at around 303.14–344.81 °C (2.31%) and 313.98–343.42 °C (2.58%). The onset of decomposition temperature for NE without extract and whit extract was 303.14 and 313.42 °C, respectively, which indicates that the thermal stability of NE whit extract increased by 10.28 °C. This showed that the NE-Opt loaded with the extract was more thermally stable than the emulsion without extract. Therefore, this increase in stability could be associated with the addition of the triterpenic extract. Triterpenic extract was relatively stable to a temperature of about 218.45 °C and decomposed totally at around 371.88 °C. Thus, the shifting of the thermal decomposition of extract to higher temperature reveals the possible interaction between the components of the emulsion and the extract (Celebioglu, Yildiz, & Uyar, 2018). Comparable trends were described by Miss-Zacarías et al. (2020) in emulsions loaded of citral.

Regarding the DSC analysis of the NE-Opt (with and without extract) and its components (Fig. 5B). The H-pan showed a glass transition temperature (Tg) of 133.31 °C and two endothermic peaks at 158.66 and 250.65 °C. The triterpenic extract showed an endothermic peak at 68.99 °C, which suggests the elimination of water and organic solvent residues during heating (Vieira-Júnior et al., 2005), a second peak was observed at 132.00 °C (between 102.24 and 132 °C) and a third endothermic event at 239.63 °C (between 207.60 and 258.96 °C) which could be are related to the melting of isomers in the extract. This thermal event matches with the weight loss due to volatilization that was recorded in the TGA (da Silva-Júnior & de Pinheiro, 2017). Olive oil showed an exothermic peak at 201.79 °C attributed to the loss of the volatile compounds with low molecular weights.

The DSC thermograms of the NE-Opt with extract and without extract displayed an endothermic peak around 168.85 and 167.64 °C, respectively. No melting peak of the extract was detected in the DSC of NE with extract. This observation evidences that extract was molecularly dispersed, that is, dissolved in the oil phase of the nanoemulsion. The absence of the extract peak or other emulsion component in the thermogram of the NE-Opt with extract indicates that occurred an interaction between the components of the emulsion and the extract (Souza, Deyse Gurak, & Marczak, 2017). This behaviour was similarly described by Aslam et al. (2016). Additionally, the NE with and without extract showed a Tg of 139.90 and 138.33 °C, respectively, these temperatures are higher than those of H-Pan, which could indicate that the protein hydrolysate improved the thermal stability of the NEs. Although there was no significant increase in the Tg of the emulsion with extract over the emulsion without extract, the effect of adding the extract to the formulation was reflected in the enthalpy of the observed endothermic peak. The enthalpy of NE with extract (1713.4 J/g) was higher than the enthalpy of NE without extract (1663.5 J/g), which would confirm the interaction of the extract with the emulsion components. Interactions and the subsequent complex formation are detected by intensity reduction (enthalpy) and/or expansion of endothermic peak when compared with the other components of the emulsion and HVBC (Souza et al., 2017).

In general, the results demonstrated that emulsions stabilized with jackfruit leaf protein hydrolysates have relatively good EE% and LD%, and comparable stability to emulsions stabilized with other sources of vegetable proteins. In this way, jackfruit leaf protein hydrolysate is a new emulsifier available for applications in the food industry. Moreover, the abundance of plants and leafy materials in various industrialized crops constitute a veritable source for the production of these protein hydrolysates, which is worthy of attention. As it is imperative to discover and explore new sustainable sources of protein, especially in non-developed countries, which would allow satisfying and/or replace the current demand of animal proteins with vegetable proteins in the agri-food sector. However, the functionality of this leaf protein hydrolysate can be enhanced by combining this protein hydrolysate with another biopolymer (polysaccharide) through complexation or conjugation and promote a wider application in the food industry.

Conclusions

Nanoemulsions loaded with pentacyclic triterpenes-rich extract and stabilized with jackfruit leaf protein hydrolysates were optimized using Box–Behnken design. The BBD and the desirability functions were effectively used to obtaining a NE-Opt through ultrasound emulsification with low values of the particle size distribution (nanometric range) and PDI. Encapsulation efficiency and extract loading, and stability of the NE-Opt in different simulated processing conditions were relatively good. However, additional studies are required to modify the NE-Opt and improve the stability in a wide range of environmental conditions. At that time, the NE-Opt developed could be used to dose/incorporate a natural extract rich in triterpenic compounds with anticancer properties into a food product. Then, H-Pan would not only be used as an alternative to conventional wall materials, but it would also generate a novel low-cost plant-protein emulsifier from agro-industrial by-products such as leaves derived from the cultivation as jackfruit.

Declaration of Competing Interest

The authors declare that they have no known competing financial interests or personal relationships that could have appeared to influence the work reported in this paper.

Acknowledgments

The authors thank CONACYT (Consejo Nacional de Ciencia y Tecnología-Mexico) for their support through the project 316948 and scholarship number 713740 granted to Carolina Calderón-Chiu and CYTED thematic network code 319RT0576..

Appendix A. Supplementary data

Supplementary data to this article can be found online at https://doi.org/10.1016/j.fochx.2021.100138.

References

Ambrosone, L., Cinelli, G., Mosca, M., & Ceglie, A. (2006). Susceptibility of water-emulsified extra virgin olive oils to oxidation. *JAOCS, Journal of the American Oil Chemists' Society., 83*(2), 165–170. https://doi.org/10.1007/s11746-006-1190-2

Anghel, M., Vlase, G., Bilanin, M., Vlase, T., Albu, P., Fuliaş, A., … Doca, N. (2013). Comparative study on the thermal behavior of two similar triterpenes from birch. *Journal of Thermal Analysis and Calorimetry, 113*(3), 1379–1385. https://doi.org/10.1007/s10973-013-3203-3

Aqil, M., Kamran, M., Ahad, A., & Imam, S. S. (2016). Development of clove oil based nanoemulsion of olmesartan for transdermal delivery: Box-Behnken design optimization and pharmacokinetic evaluation. *Journal of Molecular Liquids, 214*, 238–248. https://doi.org/10.1016/j.molliq.2015.12.077

Aslam, M., Aqil, M., Ahad, A., Najmi, A. K., Sultana, Y., & Ali, A. (2016). Application of Box-Behnken design for preparation of glibenclamide loaded lipid based nanoparticles: Optimization, in vitro skin permeation, drug release and in vivo pharmacokinetic study. *Journal of Molecular Liquids, 219*, 897–908. https://doi.org/10.1016/j.molliq.2016.03.069

Balata, G., Eassa, E., Shamrool, H., Zidan, S., & Abdo Rehab, M. (2016). Self-emulsifying drug delivery systems as a tool to improve solubility and bioavailability of resveratrol. *Drug Design, Development and Therapy, 10*, 117. https://doi.org/10.2147/DDDT.S95905

Calderón-Chiu, C., Calderón-Santoyo, M., Herman-Lara, E., & Ragazzo-Sánchez, J. A. (2021). Jackfruit (*Artocarpus heterophyllus* Lam) leaf as a new source to obtain protein hydrolysates: Physicochemical characterization, techno-functional properties and antioxidant capacity. *Food Hydrocolloids, 112*, 106319. https://doi.org/10.1016/j.foodhyd.2020.106319

Celebioglu, A., Yildiz, Z. I., & Uyar, T. (2018). Fabrication of electrospun eugenol/cyclodextrin inclusion complex nanofibrous webs for enhanced antioxidant property, water solubility, and high temperature stability. *Journal of Agricultural and Food Chemistry, 66*(2), 457–466. https://doi.org/10.1021/acs.jafc.7b04312

da Silva-Júnior, W. F., Pinheiro, J. G. de O., Moreira, C. D. L. de F. A., Rüdiger, A. L., Barbosa, E. G., Lima, E. S., da Veiga Júnior, V. F., da Silva Júnior, A. A., Aragão, C. F. S., & de Lima, Á. A. N. (2017). Thermal behavior and thermal degradation kinetic parameters of triterpene α, β amyrin. Journal of Thermal Analysis and Calorimetry, 127(2), 1757–1766. https://doi.org/10.1007/s10973-016-6046-x.

Drapala, K. P., Mulvihill, D. M., & O'Mahony, J. A. (2018). A review of the analytical approaches used for studying the structure, interactions and stability of emulsions in nutritional beverage systems. *Food Structure, 16*, 27–42. https://doi.org/10.1016/j.foostr.2018.01.004

Fasolo, D., Pippi, B., Meirelles, G., Zorzi, G., Fuentefria, A. M., von Poser, G., & Teixeira, H. F. (2020). Topical delivery of antifungal Brazilian red propolis benzophenones-rich extract by means of cationic lipid nanoemulsions optimized by means of Box-Behnken Design. *Journal of Drug Delivery Science and Technology, 56*, 101573. https://doi.org/10.1016/j.jddst.2020.101573

Fernández Sosa, E. I., Chaves, M. G., Henao Ossa, J. S., Quiroga, A. V., & Avanza, M. V. (2021). Protein isolates from Cajanus cajan L. as surfactant for o:W emulsions: pH and ionic strength influence on protein structure and emulsion stability. *Food Bioscience, 42*, 101159. https://doi.org/10.1016/j.fbio.2021.101159

Galves, C., Galli, G., Miranda, C. G., & Kurozawa, L. E. (2021). Improving the emulsifying property of potato protein by hydrolysis: An application as encapsulating agent with maltodextrin. *Innovative Food Science & Emerging Technologies, 70*, 102696. https://doi.org/10.1016/j.ifset.2021.102696

Kalam, M. A., Khan, A. A., Khan, S., Almalik, A., & Alshamsan, A. (2016). Optimizing indomethacin-loaded chitosan nanoparticle size, encapsulation, and release using Box-Behnken experimental design. *International Journal of Biological Macromolecules, 87*, 329–340. https://doi.org/10.1016/j.ijbiomac.2016.02.033

Karami, Z., Saghatchi Zanjani, M. R., & Hamidi, M. (2019). Nanoemulsions in CNS drug delivery: Recent developments, impacts and challenges. *Drug Discovery Today, 24*(5), 1104–1115. https://doi.org/10.1016/j.drudis.2019.03.021

Kentish, S., Wooster, T. J., Ashokkumar, M., Balachandran, S., Mawson, R., & Simons, L. (2008). The use of ultrasonics for nanoemulsion preparation. *Innovative Food Science & Emerging Technologies, 9*(2), 170–175. https://doi.org/10.1016/j.ifset.2007.07.005

Lam, R. S. H., & Nickerson, M. T. (2013). Food proteins: A review on their emulsifying properties using a structure–function approach. *Food Chemistry, 141*(2), 975–984. https://doi.org/10.1016/j.foodchem.2013.04.038

Ling, Z., Ai, M., Zhou, Q., Guo, S., Zhou, L., Fan, H., … Jiang, A. (2020). Fabrication egg white gel hydrolysates-stabilized oil-in-water emulsion and characterization of its stability and digestibility. *Food Hydrocolloids, 102*, 105621. https://doi.org/10.1016/j.foodhyd.2019.105621

Liu, C., Bhattarai, M., Mikkonen, K. S., & Heinonen, M. (2019). Effects of enzymatic hydrolysis of fava bean protein isolate by alcalase on the physical and oxidative stability of oil-in-water emulsions [Research-article]. *Journal of Agricultural and Food Chemistry, 67*(23), 6625–6632. https://doi.org/10.1021/acs.jafc.9b00914

McClements, D. J. (2004). Protein-stabilized emulsions. *Current Opinion in Colloid and Interface Science, 9*(5), 305–313. https://doi.org/10.1016/j.cocis.2004.09.003

Miss-Zacarías, D. M., Iñiguez-Moreno, M., Calderón-Santoyo, M., & Ragazzo-Sánchez, J. A. (2020). Optimization of ultrasound-assisted microemulsions of citral using biopolymers: Characterization and antifungal activity. *Journal of Dispersion Science and Technology, 1–10*. https://doi.org/10.1080/01932691.2020.1857264

Ozturk, B., Argin, S., Ozilgen, M., & McClements, D. J. (2015). Formation and stabilization of nanoemulsion-based vitamin E delivery systems using natural biopolymers: Whey protein isolate and gum arabic. *Food Chemistry, 188*, 256–263. https://doi.org/10.1016/j.foodchem.2015.05.005

Pan, X., Fang, Y., Wang, L., Xie, M., Hu, B., Zhu, Y., … Hu, Q. (2019). Effect of enzyme types on the stability of oil-in-water emulsions formed with rice protein hydrolysates. *Journal of the Science of Food and Agriculture, 99*(15), 6731–6740. https://doi.org/10.1002/jsfa.v99.1510.1002/jsfa.9955

Pongsumpun, P., Iwamoto, S., & Siripatrawan, U. (2020). Response surface methodology for optimization of cinnamon essential oil nanoemulsion with improved stability and antifungal activity. *Ultrasonics Sonochemistry, 60*, 104604. https://doi.org/10.1016/j.ultsonch.2019.05.021

Ramos-Bell, S., Calderón-Santoyo, M., Barros-Castillo, J. C., & Ragazzo-Sánchez, J. A. (2020). Characterization of submicron emulsion processed by ultrasound homogenization to protect a bioactive extract from sea grape (*Coccoloba uvifera* L.). *Food Science and Biotechnology, 29*(10), 1365–1372. https://doi.org/10.1007/s10068-020-00780-0

Ramos-Hernández, J. A., Calderón-Santoyo, M., Navarro-Ocaña, A., Barros-Castillo, J. C., & Ragazzo-Sánchez, J. A. (2018). Use of emerging technologies in the extraction of lupeol, α-amyrin and β-amyrin from sea grape (*Coccoloba uvifera* L.). *Journal of Food Science and Technology., 55*(7), 2377–2383. https://doi.org/10.1007/s13197-018-3152-8

Ramos-Hernández, J. A., Calderón-Santoyo, M., Burgos-Hernández, A., García- Romo, J. S., Navarro-Ocaña, A., Burboa-Zazueta, M. G., Sandoval-Petris, E., & Ragazzo-Sánchez, J. A. (2021). Antimutagenic, Antiproliferative and Antioxidant Properties of Sea Grape Leaf Extract Fractions (Coccoloba uvifera L.). Anti-Cancer Agents in Medicinal Chemistry, 21. https://doi.org/10.2174/1871520621999210104201242.

Ruiz-Montañez, G., Ragazzo-Sanchez, J. A., Picart-Palmade, L., Calderón-Santoyo, M., & Chevalier-Lucia, D. (2017). Optimization of nanoemulsions processed by high-pressure homogenization to protect a bioactive extract of jackfruit (*Artocarpus heterophyllus* Lam). *Innovative Food Science and Emerging Technologies, 40*, 35–41. https://doi.org/10.1016/j.ifset.2016.10.020

Salvador, J. A. R., Leal, A. S., Valdeira, A. S., Gonçalves, B. M. F., Alho, D. P. S., Figueiredo, S. A. C., … Mendes, V. I. S. (2017). Oleanane-, ursane-, and quinone methide friedelane-type triterpenoid derivatives: Recent advances in cancer treatment. *European Journal of Medicinal Chemistry, 142*, 95–130. https://doi.org/10.1016/j.ejmech.2017.07.013

Saravana, P. S., Shanmugapriya, K., Gereniu, C. R. N., Chae, S.-J., Kang, H. W., Woo, H.-C., & Chun, B.-S. (2019). Ultrasound-mediated fucoxanthin rich oil nanoemulsions stabilized by κ-carrageenan: Process optimization, bio-accessibility and cytotoxicity. *Ultrasonics Sonochemistry, 55*, 105–116. https://doi.org/10.1016/j.ultsonch.2019.03.014

Sarkar, A., Kamaruddin, H., Bentley, A., & Wang, S. (2016). Emulsion stabilization by tomato seed protein isolate: Influence of pH, ionic strength and thermal treatment. *Food Hydrocolloids, 57*, 160–168. https://doi.org/10.1016/j.foodhyd.2016.01.014

Sharif, H. R., Williams, P. A., Sharif, M. K., Abbas, S., Majeed, H., Masamba, K. G., … Zhong, F. (2018). Current progress in the utilization of native and modified legume proteins as emulsifiers and encapsulants – A review. *Food Hydrocolloids, 76*, 2–16. https://doi.org/10.1016/j.foodhyd.2017.01.002

Silva, H. D., Cerqueira, M. A., Souza, B. W. S., Ribeiro, C., Avides, M. C., Quintas, M. A. C., … Vicente, A. A. (2011). Nanoemulsions of β-carotene using a high-energy emulsification- evaporation technique. *Journal of Food Engineering, 102*(2), 130–135. https://doi.org/10.1016/j.jfoodeng.2010.08.005

Souza, A. C. P., Deyse Gurak, P., & Damasceno Ferreira Marczak, L. (2017). Maltodextrin, pectin and soy protein isolate as carrier agents in the encapsulation of anthocyanins-rich extract from jaboticaba pomace. Food and Bioproducts Processing, 102, 186–194. https://doi.org/10.1016/j.fbp.2016.12.012.

Taha, A., Ahmed, E., Ismaiel, A., Ashokkumar, M., Xu, X., Pan, S., & Hu, H. (2020). Ultrasonic emulsification: An overview on the preparation of different emulsifiers-stabilized emulsions. *Trends in Food Science & Technology, 105*, 363–377. https://doi.org/10.1016/j.tifs.2020.09.024

Tang, S. Y., Manickam, S., Wei, T. K., & Nashiru, B. (2012). Formulation development and optimization of a novel Cremophore EL-based nanoemulsion using ultrasound cavitation. *Ultrasonics Sonochemistry, 19*(2), 330–345. https://doi.org/10.1016/j.ultsonch.2011.07.001

Vieira-Júnior, G. M., de Souza, C. M. L., & Chaves, M. H. (2005). Resina de Protium heptaphyllum: Isolamento, caracterização estrutural e avaliação das propriedades

térmicas. *Química Nova, 28*(2), 183–187. https://doi.org/10.1590/S0100-40422005000200003

Xu, Xingfeng, Liu, Wei, Liu, Chengmei, Luo, Liping, Chen, Jun, Luo, Shunjing, … Wu, Lixin (2016). Effect of limited enzymatic hydrolysis on structure and emulsifying properties of rice glutelin. *Food Hydrocolloids, 61*, 251–260. https://doi.org/10.1016/j.foodhyd.2016.05.023

Yasir, M., & Sara, U. V. S. (2013). Preparation and optimization of haloperidol loaded solid lipid nanoparticles by Box-Behnken design. *Journal of Pharmacy Research, 7*(6), 551–558. https://doi.org/10.1016/j.jopr.2013.05.022

Zang, X., Yue, C., Wang, Y., Shao, M., & Yu, G. (2019). Effect of limited enzymatic hydrolysis on the structure and emulsifying properties of rice bran protein. *Journal of Cereal Science, 85*, 168–174. https://doi.org/10.1016/j.jcs.2018.09.001